Gas Adsorption on Heterogeneous Single-Walled Carbon Nanotube Bundles

Wei Shi and J. Karl Johnson*

Department of Chemical and Petroleum Engineering, University of Pittsburgh, Pittsburgh, Pennsylvania 15261, USA and National Energy Technology Laboratory, Pittsburgh, Pennsylvania 15236, USA

(Received 22 April 2003; published 3 July 2003)

Optimization of carbon nanotube bundles containing a distribution of nanotube diameters always gives structures with packing defects that form relatively large interstitial channels. Experimental data for CH_4, Ar, and Xe adsorption are compared with simulations. Low coverage experimental isosteric heats are in excellent agreement with simulations of gases adsorbing into interstitial channels of defective nanotube bundles, whereas adsorption onto perfect bundles does not agree with experiments. Thus, an accurate description of adsorption on nanotube bundles must account for interstitial adsorption.

DOI: 10.1103/PhysRevLett.91.015504 PACS numbers: 68.43.Fg, 61.46.+w, 67.70.+n, 82.60.–s

Single-walled carbon nanotubes (SWNTs) are of interest as gas adsorbents because of their unique structural properties. Four different adsorption sites have been identified on bundles of SWNTs: internal (endohedral), interstitial channels (ICs), external groove sites, and external surfaces [1,2]. Experimental gas adsorption data on SWNT bundles have previously been analyzed in terms of an oversimplified model of homogeneous nanotubes (all the same diameter) packed into perfect arrays. This analysis has led to the general conclusion that gases do not adsorb inside ICs [1,3]. Real SWNT bundles contain SWNTs with a variety of different diameters (heterogeneous). Here we show that realistic nanotube bundles exhibit packing defects resulting in large ICs. We use atomistic simulations to compute adsorption of CH_4, Ar, and Xe onto both homogeneous and heterogeneous SWNT bundles. These simulations show that gases as large as Xe do adsorb into defect ICs of heterogeneous bundles. Reexamination of experimental data [3–12] shows that heats of adsorption are in remarkably good agreement with simulations of adsorption onto heterogeneous bundles and not with homogeneous bundles. Thus, adsorption inside ICs of SWNT bundles is required to accurately describe these materials.

It is well known that nanotube bundles contain a distribution of different nanotube diameters [13–17]. However, virtually all previous simulations and theoretical analyses of experimental data have assumed a perfect array of homogeneous bundles. We have generated atomistic models of both homogeneous and heterogeneous SWNT bundles containing from 45 to 100 tubes. The tube diameters in the heterogeneous bundles were chosen to resemble the diameter distributions measured in experiments [16]. Homogeneous bundles were constructed of (10,10) SWNTs, where n,m represents the indices that define the nanotube diameter and chirality [18]. The initial positions of the nanotubes were chosen randomly with the constraint that none of the tubes overlap [19]. The tube positions were optimized using the basin-hopping method [20–22]. Examples of optimized homogeneous and heterogeneous bundles containing 45 nanotubes are shown in Fig. 1. Optimization of homogeneous bundles results in packing of the tubes into perfect 2D hexagonal lattices, while optimized heterogeneous bundles *always* contain multiple packing defects that give comparatively large ICs. This key result shows that the basin-hopping method is capable of finding near-global minima for tube packing, as is evident from the hexagonal packing of homogeneous bundles. It also indicates that real bundles must contain a number of packing defects that give rise to relatively large ICs. The heterogeneous bundle in Fig. 1 contains 10 (8,8), 25 (9,9), 5 (10,10), and 5 (11,11) nanotubes, giving an average diameter of 12.4 Å and a standard deviation of 1.2 Å, which is much smaller than the 2 Å standard deviation calculated from the detailed analysis of the types of SWNT bundles used in many experiments [13]. We therefore expect our models to exhibit fewer defects than real SWNT bundles.

We have performed grand canonical Monte Carlo simulations [23] to study the adsorption of CH_4, Xe, and Ar onto bundles of closed-ended SWNTs. The

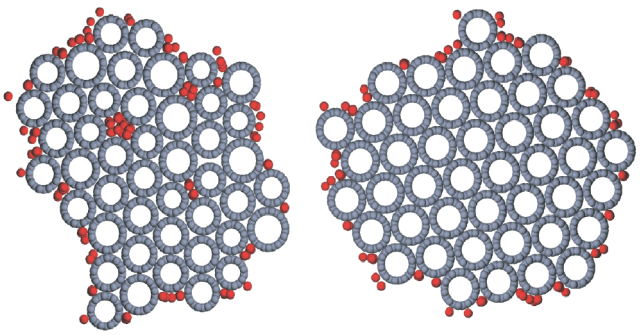

FIG. 1 (color online). Sample heterogeneous (left panel) and homogeneous (right panel) bundles optimized by the basin-hopping technique [20–22]. The red spheres represent CH_4 adsorbed in equilibrium with a bulk phase at 159.88 K and 0.05 bar.

Lennard-Jones potential was used to model fluid-fluid and solid-fluid interactions. The parameters are $\sigma_x = 3.4$, 3.81, 3.4, and 4.1 Å and $\epsilon_x/k = 28$, 148.1, 120, and 221 K, for $x =$ C, CH_4, Ar, and Xe, respectively, where k is the Boltzmann constant. Lorentz-Berthelot combining rules were applied and the parameter values were taken from the literature [1,24,25]. Binding energies for the gases on graphite from the potentials (experiments) are -11.4 (-12.2), -9.1 (-9.2), and -15.2 (-15.6) kJ mol^{-1} for CH_4, Ar, and Xe, respectively. The experimental data were reported by Vidali *et al.* [26]. The excellent agreement between the model and experimental data indicates that these parameters are a good first approximation to the fluid-nanotube interaction potential. Our molecular simulations confirm the assumption that CH_4, Ar, and Xe do not adsorb into the ICs of homogeneous bundles (see Fig. 1). Simulations also show that all heterogeneous bundles we have constructed contain large ICs at packing defect sites that do allow adsorption of all three probe molecules. For example, CH_4 is shown to adsorb in four interstitial defect sites in the left side of Fig. 1, while no interstitial adsorption is found for the homogeneous bundle on the right.

Experimental [5,7] and simulation isosteric heats of adsorption (q_{st}) data for CH_4 are plotted in Fig. 2. The coverage was computed from the known weight of the sorbent and an estimated purity of 60% [8]. The inset shows the low coverage region. This low coverage region has been assigned to adsorption into the groove sites of SWNT bundles [3,7]. The simulation data for groove site

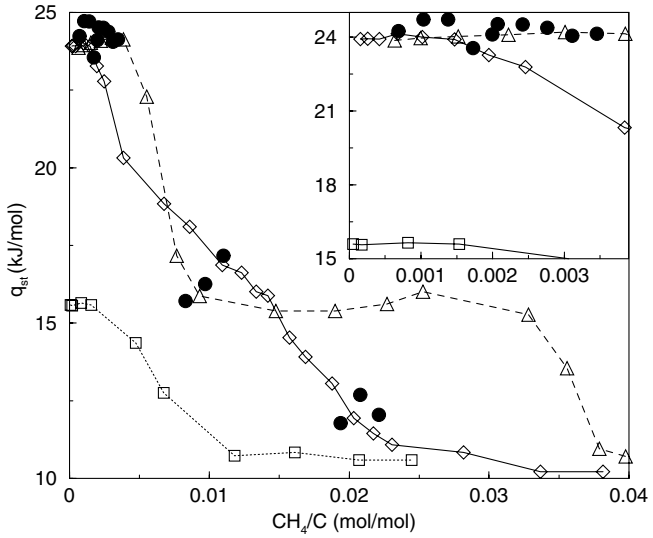

FIG. 2. Isosteric heats of adsorption for CH_4 from experiments [5,7] (circles) and simulations. The diamonds (squares) are for adsorption onto heterogeneous (homogeneous) bundles. The triangles are for a homogeneous bundle with the solid-fluid potential increased by 45%. The inset shows the low coverage region. The lines are drawn as a guide to the eye. The estimated error bars for simulations are about the size of the symbols.

adsorption on homogeneous tubes give q_{st} about 40% lower than values from experiments. In contrast, q_{st} for adsorption in the ICs of heterogeneous bundles are in good qualitative and quantitative agreement with experiments.

One might argue that the nanotube-gas (solid-fluid) interaction potential is not accurately known and that q_{st} for homogeneous bundles could be brought into agreement with experimental data by adjusting the solid-fluid potential. We have empirically increased the solid-fluid potential to bring the low coverage q_{st} from simulations on homogeneous bundles into agreement with experiment. We found that the magnitude of the potential must be increased by 45% to match experiments in the low coverage region. Isosteric heat data for this system are shown as triangles in Fig. 2. As can be seen from the inset, the agreement at low coverage is excellent. However, at high coverage, corresponding to complete monolayer formation on the external surface of the nanotubes, the simulated q_{st} values are at least 25% too high compared with experiments. In contrast, the monolayer heats from both homogeneous and heterogeneous bundles are in fairly good agreement with experiments. This analysis suggests that the assumed solid-fluid potential is relatively accurate and that only adsorption onto heterogeneous bundles, including interstitial adsorption, is consistent with experimental data.

Muris *et al.* [4] identified two steps in experimental isotherms of CH_4 adsorption on closed nanotubes, one corresponding to low coverage and another to high coverage. They estimated $q_{st} = 18.3 \pm 1$ and 11.2 ± 0.5 kJ mol^{-1} for low and high coverages, respectively. Talapatra and Migone [7] pointed out that the low coverage data from Muris *et al.* corresponds to the intermediate coverage range of their data, or around 0.01 CH_4/C in Fig. 2. Thus, the data of Muris *et al.* are in good agreement with both the experimental data of Talapatra and Migone [7] and our simulation data. The high coverage datum from Muris and co-workers is likewise in good agreement with the highest coverage region in Fig. 2 for simulations on heterogeneous bundles and experimental data. Thus, q_{st} values computed from adsorption on heterogeneous bundles are in good agreement with all available experimental data, while simulations on homogeneous nanotubes are not consistent with the totality of the data.

Isosteric heats for Ar on closed SWNT bundles have been reported by Wilson *et al.* [9] and by Talapatra *et al.* [12] over a range of coverages. We have assumed a purity of 60% for these experiments, the same as in the studies of Migone *et al.* [8], because the nanotubes in each of these studies were obtained from the same source. The isosteric heats for Ar from simulations and experiments are plotted in Fig. 3. The experimental data from Wilson *et al.* [9], shown as circles in Fig. 3, were derived from isotherms at average temperatures around 90 K. The

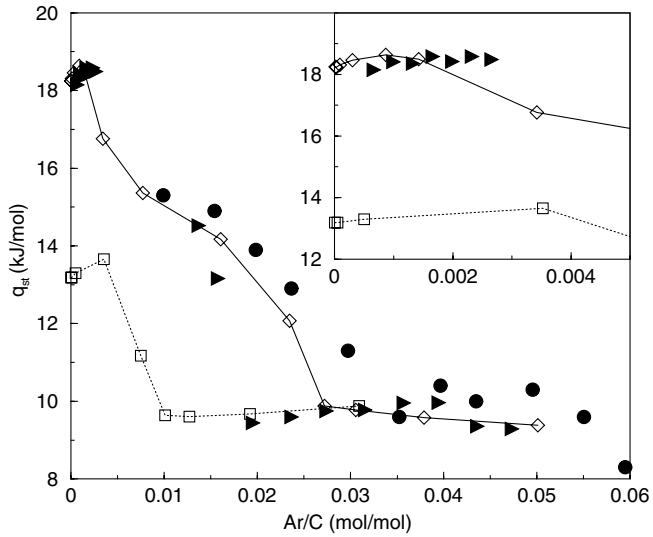

FIG. 3. Experimental and simulated q_{st} for Ar on SWNT bundles. Circles and right triangles are experimental data from Wilson *et al.* [9] and Talapatra *et al.* [12], respectively. The diamonds (squares) are simulation data for adsorption onto heterogeneous (homogeneous) bundles. The inset shows the low coverage region.

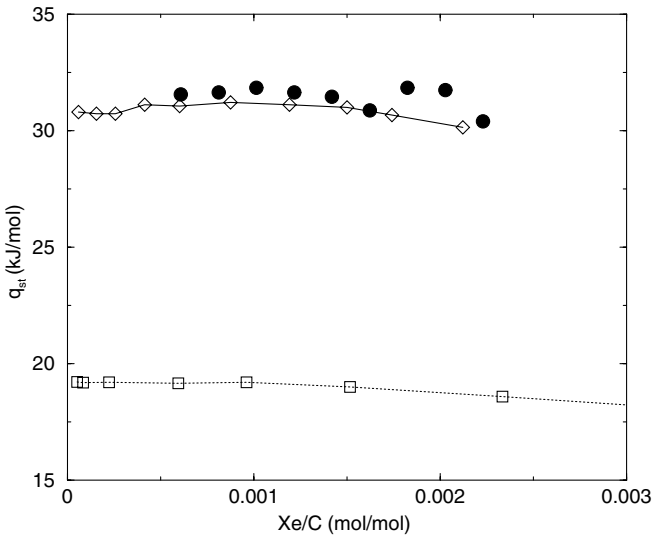

FIG. 4. Xenon q_{st} from experiments [8] (circles) and simulations on homogeneous (squares) and heterogeneous (diamonds) bundles.

experimental data of Talapatra *et al.* [12], shown as right triangles, cover a wider temperature range. The lowest coverage data correspond to temperatures from about 110 to 160 K, while the high coverage data were measured between 57 and 87 K. The simulation data were collected at 90 K. We see from Fig. 3 that the data for heterogeneous bundles are in very good agreement with both sets of experiments. The values of q_{st} from simulations on homogeneous bundles are not in good agreement with the experimental data. The inset in Fig. 3 shows the low coverage region. This region is dominated by interstitial adsorption for the heterogeneous bundles, and the excellent agreement between simulations and the data of Talapatra *et al.* is evidence that interstitial adsorption dominates the behavior of q_{st} in the experiments at low coverage. Simulations of homogeneous bundles give q_{st} values about 25% too low compared with experiments.

The heat of adsorption or binding energy of Xe on closed SWNT bundles has been determined experimentally by at least three different groups [3,8,10,11]. Only one of these groups reported q_{st} as a function of coverage [8]. These data are plotted in Fig. 4 along with simulation results at 250 K. The experimental data are from isotherms over a range of temperatures from 210 to 295 K at very low coverage. The agreement between simulations and experiments is remarkable for the heterogeneous bundles. The simulations on homogeneous bundles give q_{st} values about 40% too low. Talapatra *et al.* [3] report a binding energy of $-27.2\ \mathrm{kJ\,mol^{-1}}$ based on isotherms from 220 to 295 K, in excellent agreement with that measured from thermal desorption spectroscopy of $-27\ \mathrm{kJ\,mol^{-1}}$ at around 100 K [10] Using the formula $q_{st} = -\epsilon + \alpha kT$ where ϵ is the binding energy, $\alpha = 0.5$ for 2D systems and 2 for 1D systems [9], we find $q_{st} = 31.2\ \mathrm{kJ\,mol^{-1}}$ at 250 K, in excellent agreement with both experiments from Zambano *et al.* [8] and our simulations on heterogeneous bundles. Muris and co-workers measured $q_{st} = 15.7\ \mathrm{kJ\,mol^{-1}}$ and Talapatra and Migone [6] reported $q_{st} = 16.6\ \mathrm{kJ\,mol^{-1}}$ for coverages corresponding to full monolayer completion. These values are in reasonably good agreement with simulations on both the homogeneous and heterogeneous bundles near monolayer completion (not shown). This is to be expected, since the external surfaces of the nanotubes are not sensitive to the diameter distribution or packing defects in the bundles.

The overall agreement between simulations and experiments clearly indicates that gases as large as Xe do adsorb in the ICs that result from packing defects in real nanotube bundles. This finding contradicts a previous analysis of experimental data and previous theoretical calculations based on a model of SWNT bundles consisting of perfectly packed homogeneous nanotubes [1,3,7,8]. Plots of q_{st} at low coverage for CH_4, Ar, and Xe from experiments show a measurable plateau region. This plateau directly corresponds to adsorption in ICs in the simulations. Simulations on a variety of different heterogeneous bundles indicate that highly optimized bundles contain only a few defect ICs that allow gas adsorption. Such bundles have plateau regions that are more narrow than those observed in experiments, while still giving values of q_{st} at the lowest coverages that agree with experiments. The heterogeneous simulation data reported in this paper are for a 45 nanotube bundle that is less optimized than that shown in Fig. 1 and contains several more defect ICs. This bundle was produced by making only a few optimization steps in the basin-hopping method. Simulations on highly

optimized bundles containing 100 nanotubes give plateau regions in agreement with experimental data. This indicates that either the SWNT bundles used in the experiments contain more tubes than previously estimated [11,13] or more defects than our highly optimized bundles. The larger number of defects in real bundles may be due to the larger standard deviation of nanotube diameters observed in real bundles [13].

We observe from simulations that the groove sites on homogeneous bundles also produce a plateau region in the q_{st} versus coverage plots (see Figs. 2–4). This plateau region for groove site filling occurs at lower q_{st} values than IC filling of heterogeneous bundles. However, there is no obvious plateau region corresponding to groove site filling for the heterogeneous bundles for CH_4 and Ar (see Figs. 2 and 3). This is because the groove site plateau region is convoluted with adsorption that occurs in the higher energy interstitial sites; i.e., q_{st} for heterogeneous bundles in the coverage range where groove sites are filling is an average of contributions from some partially filled ICs and some groove sites. While there is a distribution of groove site binding energies, the distribution appears to be quite narrow. We have observed that the groove sites for both homogeneous and heterogeneous bundles are very similar [27].

J. K. J. acknowledges support from the National Science Foundation, Grant No. CTS-9702239. We thank M. W. Cole, O. E. Vilches, A. D. Migone, and M. Bienfait for helpful discussions and X. C. Zhao for help with some of the calculations.

*Electronic address: karlj@pitt.edu

[1] G. Stan *et al.*, Phys. Rev. B **62**, 2173 (2000).
[2] K. A. Williams and P. C. Eklund, Chem. Phys. Lett. **320**, 352 (2000).
[3] S. Talapatra, A. Z. Zambano, S. E. Weber, and A. D. Migone, Phys. Rev. Lett. **85**, 138 (2000).
[4] M. Muris *et al.*, Langmuir **16**, 7019 (2000).
[5] S. E. Weber *et al.*, Phys. Rev. B **61**, 13150 (2000).
[6] S. Talapatra and A. D. Migone, Phys. Rev. Lett. **87**, 206106 (2001).
[7] S. Talapatra and A. D. Migone, Phys. Rev. B **65**, 045416 (2002).
[8] A. J. Zambano, S. Talapatra, and A. D. Migone, Phys. Rev. B **64**, 075415 (2001).
[9] T. Wilson *et al.*, J. Low Temp. Phys. **126**, 403 (2002).
[10] H. Ulbricht, J. Kriebel, G. Moos, and T. Hertel, Chem. Phys. Lett. **363**, 252 (2002).
[11] M. Muris, N. Dupont-Pavlovsky, M. Bienfait, and P. Zeppenfeld, Surf. Sci. **492**, 67 (2001).
[12] S. Talapatra, D. S. Rawat, and A. D. Migone, J. Nanosci. Nanotech. **2**, 467 (2002).
[13] S. Rols *et al.*, Eur. Phys. J. B **10**, 263 (1999).
[14] S. Bandow *et al.*, Phys. Rev. Lett. **80**, 3779 (1998).
[15] A. M. Rao *et al.*, Science **275**, 187 (1997).
[16] A. G. Rinzler *et al.*, Appl. Phys. A **67**, 29 (1998).
[17] J. W. G. Wildoer *et al.*, Nature (London) **391**, 59 (1998).
[18] *Science of Fullerines & Carbon Nanotubes*, edited by M. S. Dresselhaus, G. Dresselhaus, and P. C. Eklund (Academic Press, Inc., San Diego, 1996).
[19] M. R. Smith, Jr. *et al.*, J. Phys. Chem. B **107**, 3752 (2003).
[20] D. J. Wales and J. P. K. Doye, J. Phys. Chem. A **101**, 5111 (1997).
[21] J. P. K. Doye and D. J. Wales, Phys. Rev. Lett. **80**, 1357 (1998).
[22] D. J. Wales and H. A. Scheraga, Science **285**, 1368 (1999).
[23] M. P. Allen and D. J. Tildesley, *Computer Simulation of Liquids* (Clarendon, Oxford, 1987).
[24] W. A. Steele, Surf. Sci. **36**, 317 (1973).
[25] S. Y. Jiang, K. E. Gubbins, and J. A. Zollweg, Mol. Phys. **80**, 103 (1993).
[26] G. Vidali, G. Ihm, H. Y. Kim, and M. W. Cole, Surf. Sci. Rep. **12**, 133 (1991).
[27] W. Shi and J. K. Johnson (to be published).